

# Detection of the Microvascular Changes of Diabetic Retinopathy Progression Using Optical Coherence Tomography Angiography

Xiaogang Wang<sup>1,\*</sup>, Yongqing Han<sup>2,\*</sup>, Gang Sun<sup>3</sup>, Fang Yang<sup>4</sup>, Wen Liu<sup>4</sup>, Jing Luo<sup>5</sup>, Xing Cao<sup>5</sup>, Pengyi Yin<sup>5</sup>, Frank L. Myers<sup>6</sup>, and Liang Zhou<sup>5</sup>

<sup>1</sup> Department of Ophthalmology, Shanxi Eye Hospital, Taiyuan, Shanxi, P.R. China

<sup>2</sup> Department of Ophthalmology, The Affiliated Hospital of Inner Mongolia Medical University, Hohhot, Inner Mongolia, P.R. China

<sup>3</sup> College of electrical and information engineering, Hunan University, Changsha, Hunan, P.R. China

<sup>4</sup> Department of Epidemiology and Health Statistics, Xiangya School of Public Health, Central South University, Changsha, Hunan, P.R. China

<sup>5</sup> Department of Ophthalmology, the Second Xiangya Hospital, Central South University, Changsha, Hunan, P.R. China

<sup>6</sup> Department of Ophthalmology and Visual Sciences, University of Wisconsin-Madison School of Medicine and Public Health, Madison, WI, USA

**Correspondence:** Liang Zhou, Department of Ophthalmology, The Second Xiangya Hospital, Central South University, 139 Middle Renmin Road, Hunan 410011, P.R. China. e-mail: [zhouliang12@csu.edu.cn](mailto:zhouliang12@csu.edu.cn)

**Received:** March 26, 2021

**Accepted:** May 9, 2021

**Published:** June 30, 2021

**Keywords:** diabetic retinopathy; optical coherence tomography angiography; vessel density; extrafoveal avascular area; vessel diameter index

**Citation:** Wang X, Han Y, Sun G, Yang F, Liu W, Luo J, Cao X, Yin P, Myers FL, Zhou L. Detection of the microvascular changes of diabetic retinopathy progression using optical coherence tomography angiography. *Transl Vis Sci Technol.* 2021;10(7):31, <https://doi.org/10.1167/tvst.10.7.31>

**Purpose:** To investigate microvascular parameters that are related to the severity of diabetic retinopathy (DR) with optical coherence tomography angiography (OCTA).

**Methods:** In total, 105 eyes from 105 diabetic patients were recruited in this prospective cross-sectional study, including 37 eyes with no clinical signs of DR (NoDR), 43 eyes with nonproliferative diabetic retinopathy (NPDR), and 25 eyes with proliferative diabetic retinopathy (PDR). Angiogram images from the parafoveal superficial capillary plexus (SCP), the deep capillary plexus (DCP), and the radial peripapillary capillary plexus were analyzed, and metrics were compared among groups. Multivariate regression analysis was used to identify the best OCTA parameters that could distinguish DR severity among groups.

**Results:** Parafoveal vessel diameter index in the SCP and vessel density (VD) in the DCP showed the strongest correlation with the severity of DR ( $P < 0.01$ ). Extrafoveal avascular area in the SCP was the parameter that could most distinguish NoDR from NPDR ( $P < 0.01$ ) with sensitivity and specificity of 83.72% and 78.38%, respectively. VD in the DCP also was the most sensitive biomarker to distinguish NPDR from PDR ( $P < 0.01$ ) with sensitivity and specificity of 84.00% and 79.07%, respectively.

**Conclusions:** The microvascular changes in the SCP and DCP in DR may have different characteristics that could be identified with specific OCTA parameters. OCTA serves as a promising technology to discriminate eyes with different severity of DR.

**Translational Relevance:** Our study investigated OCTA metrics and severity of DR. At different stages of DR, ophthalmologists may focus on specific OCTA parameters to predict the progression of retinopathy in individual patients.

## Introduction

Diabetes is a common metabolic disease that involves multiple organs in working-age adults. The prevalence of diabetes mellitus worldwide was 422 million individuals in 2014, and China accounted for 24.4% of the total.<sup>1</sup> As one of the most severe

complications of diabetes, the prevalence of diabetic retinopathy (DR) was estimated to increase from 126 million in 2010 to 191 million by 2030 worldwide, especially in those areas with poor education and health screening systems.<sup>2</sup> The pathogenic progression of DR begins as loss of pericytes in the capillary wall, which leads to retinal capillary microaneurysms formation with hard exudates.<sup>3</sup> Intraretinal

hemorrhages and cotton-wool spots then start to appear if the blood sugar is still uncontrolled. In the proliferative stage, the concentration of vascular endothelial growth factor (VEGF) increases, and neovascularization can occur, which may result in vitreous hemorrhage and neovascular glaucoma. Up to now, the grading and risk assessment of DR is largely based on color fundus photography and fluorescein angiography (FA).<sup>4</sup>

Optical coherence tomography angiography (OCTA) is a rapid and noninvasive technique that can visualize microvasculature of the retina *in vivo*.<sup>5</sup> It has been used in observing DR of different severity from the subtle changes of preclinical diabetic retinopathy to the retinal neovascularization of PDR. OCTA technologies in the macular scan automatically segment the retinal capillaries into the superficial capillary plexus (SCP) and the deep capillary plexus (DCP). Likewise, in the optic disc scan, the radial peripapillary capillary plexus (RPCP) can be identified. OCTA not only can identify the FA-based criteria such as areas of nonperfusion, microaneurysms, and neovascularization, but also has its specific parameters such as FD-300, vessel density, and more that can be quantified and statistically analyzed.<sup>6,7</sup> The sensitivity and specificity of some of these parameters have been studied previously. In this study, we compared overall 18 metrics in the parafoveal SCP, DCP, and peripapillary RPCP in diabetic retinas with different severity to identify the ideal biomarkers that could detect the progression of retinopathy.

## Methods

This is a prospective cross-sectional study analyzing OCTA images and comparing the metric data between diabetic groups with different DR severity. The patients' demographic data and angiogram images were collected from the Affiliated Hospital of Inner Mongolia University for the Nationalities. The study protocol was approved by the Medical Ethics Committee of Affiliated Hospital of Inner Mongolia University for the Nationalities in accordance with the principles of the Declaration of Helsinki. Written informed consent was obtained from all study participants.

## Participants

A total of 105 eyes of 105 participants with type 2 diabetes mellitus were included in this study. There were 37 diabetic eyes with no clinical signs of

DR (NoDR), 43 eyes with nonproliferative diabetic retinopathy (NPDR) and 25 eyes with proliferative diabetic retinopathy (PDR). Exclusion criteria included (1) intraocular pressure higher than 21 mm Hg (evaluated using non-contact tonometer) or any types of glaucoma; (2) quality score of images below six (10 as full score), inaccurate segmentation of the retinal layers or slabs, motion artifacts, shadow or blur of the image, or poor fixation by the patients; (3) patients with astigmatism (more than 2 diopters), or refractive error (myopia more than 2 diopters, hyperopia more than 1 diopter); (4) history of panretinal photocoagulation, intravitreal injection or any ocular surgeries; (5) patients with diabetic macular edema (central retinal thickness greater than 300  $\mu\text{m}$ ); (6) patients with retinal diseases other than diabetic retinopathy; (7) patients with neurologic diseases other than diabetic neuropathy.

All patients included in the study were checked for best-corrected visual acuity (BCVA), and intraocular pressure. Fundus examination and OCTA were then performed. Patients with microaneurysms or hemorrhages underwent fluorescein angiography to classify NPDR and PDR in accordance with the guidelines.<sup>4</sup> Duration of diabetes mellitus was recorded. BCVA was determined for all subjects using Tumbling E charts and converted to logMAR for statistical analysis.

## OCTA Imaging

All the participants underwent an OCTA scan using the RTVue-XR Avanti system (Optovue, Inc., Fremont, CA, USA). The  $3 \times 3$  mm AngioRetina scans centered on the fovea and  $4.5 \times 4.5$  mm AngioDisc scans centered on the optic nerve head were obtained for each patient.

The slabs of SCP, DCP, and RPCP were automatically segmented by the built-in software (RTVue XR, Version 2018.1.0.43; Optovue, Fremont, CA, USA). The segmentations were checked manually by two experienced retinal specialists and images with inaccurate segmentation were excluded from the study. SCP was defined as the retinal layer between the inner limiting membrane (ILM) and 10  $\mu\text{m}$  above the inner plexiform layer (IPL). DCP was defined as the retinal layer between 10  $\mu\text{m}$  above the IPL and 10  $\mu\text{m}$  below the outer plexiform layer (OPL). RPCP was defined as the layer between the ILM and the posterior boundary of the retinal nerve fiber layer (RNFL). To avoid projections of large vessels from the superficial layer of the retina, the new algorithm of projection artifact removal was used in the updated Optovue equipment.<sup>8</sup>

## Quantification of Retinal Microvasculature

All OCTA images were analyzed with the MATLAB program (R2017a, version 9.2.0.538062). Foveal avascular zone (FAZ) metrics including the FAZ area, FAZ perimeter, acircularity index (AI) and the FD-300 were assessed for the combined SCP and DCP. Vessel density (VD), extrafoveal avascular area (EAA) and vessel morphology metrics including vessel length fraction (VLF), fractal dimension and vessel diameter index (VDI) were assessed for the SCP and DCP respectively in the  $3 \times 3$  mm macular scans. VD, VLF, fractal dimension and VDI were assessed for the RPCP in the  $4.5 \times 4.5$  mm disc scans. The delineation of the FAZ was checked by a retinal specialist, and images with inaccurate segmentation were analyzed manually with MATLAB. VD for the  $3 \times 3$  mm macular scans was assessed in an annular area with inner and outer ring diameters of 1mm and 3mm both centered on the fovea. VD for the  $4.5 \times 4.5$  mm optic disc scans was assessed in an annular area with inner and outer ring diameters of 2mm and 4mm both centered on the center of the disc.

FD-300 is defined as foveal vessel density of the  $300\mu\text{m}$  width ring surrounding the FAZ. To obtain the FD-300, the  $300\mu\text{m}$  width ring is first located and then vessel density within the ring was calculated as previously described.<sup>9</sup>

EAA is calculated as the percentage of avascular area outside a 1-mm circle with the same center point of the image which has previously been described.<sup>10</sup> Briefly, first, obtain the threshold of the vessel distance map, then apply erosion operations to the vessel distance map with a five-pixel-wide square kernel, eliminate areas smaller than eight pixels in the vessel distance map, and then apply dilation operations by a seven-pixel-wide square kernel.

VLF measures retinal vessel length. VDI measures the averaged vessel caliber. To analyze these two parameters, skeletonized images were obtained by extracting the centerline of blood vessels. The VLF was then calculated by dividing the vessel centerline pixels by total pixels, the VDI was calculated by dividing total vascular pixels by vessel centerline pixels. It should be noted that, for optic disc images, large vessels were removed by the method described in the reference, and only the small vessels within a 2mm width ring surrounding the image center were calculated. In contrast, for  $3 \times 3$  mm macular images, no large vessels were excluded from the calculation. The methods were modified from previous publications.<sup>11,12</sup>

Fractal dimension (FD) reflects the geometry and complexity of retinal vessel branching architecture. The fractal dimension was calculated over the skele-

tonized image using a box counting technique that has been reported in the literature.<sup>13</sup>

## Statistical Analysis

Statistical analysis was performed using software (SPSS for Windows, IBM, version 23.0). To compare parameters across the three groups (NoDR, NPDR, and PDR), one-way analysis of variance was used for the quantitative variables, and the  $\chi^2$  test was used for the categorical data. Variables that were statistically significant in the univariate analysis were included in an ordinal regression model for the comparison of all three DR groups or a binary logistic regression model for the comparison between two groups (NoDR vs. NPDR, NPDR vs. PDR) after the correlation test. A two-sided  $P$  value = 0.05 was used to test for statistical significance.

## Results

A total of 105 eyes of 105 patients were included in this study, consisting of 37 eyes with NoDR, 43 eyes with NPDR, and 25 eyes with PDR. There was no significant difference between age or scan quality (both 3 mm and 4.5 mm scan) among groups. The LogMar BCVA was significantly increased with the severity of DR ( $0.0351 \pm 0.0538$ ,  $0.0930 \pm 0.1183$ ,  $0.2504 \pm 0.2630$ , respectively; all  $P < 0.05$ ). Duration of DM was only statistically different between NoDR and NPDR groups ( $5.41 \pm 4.17$  vs.  $9.73 \pm 6.14$ ;  $P < 0.001$ ).

## Univariate Analysis of OCTA Parameters

OCTA metrics were compared in Table 1. FAZ area was not significantly different between groups, while the FD-300 was statistically decreased with the severity of DR ( $48.7305 \pm 3.7626$ ,  $46.8523 \pm 4.17907$ ,  $44.3060 \pm 3.7697$ ;  $P < 0.001$ ). Parameters in the SCP were significantly different between NoDR and NDPR groups (all  $P < 0.01$ ); however, these metrics were not significantly different between NPDR and PDR (all  $P > 0.05$ ) except VDI ( $P = 0.029$ ). All parameters in the DCP showed significant changes with the severity of DR ( $P < 0.05$ ) except VDI ( $P = 0.447$ ). Two parameters in the peripapillary RPCP showed significant change between NoDR and NPDR groups (VLF and VDI; both  $P < 0.05$ ) but not between NPDR and PDR groups.

**Table 1.** Demographic Characteristics and Univariate Analysis of Parameters Among the Three Groups With Severity of DR and Between Two Groups

	NoDR (37 Eyes, Mean ± SD)	NPDR (43 Eyes, Mean ± SD)	PDR (25 Eyes, Mean ± SD)	<i>P</i> <sup>*</sup>	<i>P</i> <sup>†</sup>	<i>P</i> <sup>‡</sup>
Demographic characteristics						
Sex				0.565	0.847	0.383
Male	24(64.9%)	27(62.8%)	13(52%)			
Female	13(35.1%)	16(37.2%)	12(48%)			
Age, y	50.46 ± 9.98	53.14 ± 7.61	50.80 ± 7.62	0.323	0.178	0.226
LogMar	0.0351 ± 0.05383	0.093 ± 0.11831	0.2520 ± 0.2663	<0.001	0.008	0.008
Duration, y	5.4135 ± 4.1741	9.7326 ± 6.1396	10.2800 ± 4.8263	<0.001	<0.001	0.704
SQ (3 × 3mm)	8.6486 ± 0.9780	8.3721 ± 0.8458	8.0800 ± 0.8622	0.053	0.179	0.177
SQ (4.5 × 4.5mm)	8.5676 ± 0.9292	8.5581 ± 0.7336	8.3200 ± 0.9000	0.460	0.960	0.240
FAZ associated parameters (3 mm × 3 mm)						
FAZ area, mm <sup>2</sup>	0.3204 ± 0.1221	0.3597 ± 0.1142	0.4016 ± 0.1616	0.056	0.141	0.216
PERIM, mm	2.2581 ± 0.4358	2.4742 ± 0.4429	2.6398 ± 0.5897	0.009	0.031	0.194
AI	1.1461 ± 0.0445	1.18165 ± 0.0687	1.1980 ± 0.0635	0.003	0.007	0.335
FD-300, %	48.7305 ± 3.7626	46.8523 ± 4.1791	44.306 ± 3.7697	<0.001	0.039	0.015
Superficial retinal layer (3 mm × 3 mm)						
EAA, mm <sup>2</sup>	0.0017 ± 0.0025	0.0187 ± 0.0234	0.03135 ± 0.0388	<0.001	<0.001	0.148
VD, %	48.0889 ± 4.6280	43.3233 ± 6.2583	41.4160 ± 5.5619	<0.001	<0.001	0.212
VLF	0.0684 ± 0.0075	0.0593 ± 0.0103	0.0549 ± 0.0091	<0.001	<0.001	0.083
FD	1.7471 ± 0.0140	1.7286 ± 0.0233	1.7208 ± 0.0225	<0.001	<0.001	0.181
VDI	7.0506 ± 0.2765	7.3554 ± 0.4188	7.59998 ± 0.4612	<0.001	<0.001	0.029
Deep retinal layer (3 mm × 3 mm)						
EAA, mm <sup>2</sup>	0.0006 ± 0.0019	0.0030 ± 0.0098	0.0064 ± 0.0107	0.029	0.147	0.190
VD, %	44.5893 ± 4.3004	41.3593 ± 4.6452	35.6832 ± 4.0959	<0.001	0.002	<0.001
VLF	0.0811 ± 0.0079	0.0725 ± 0.0102	0.0616 ± 0.0082	<0.001	<0.001	<0.001
FD	1.7458 ± 0.0123	1.7338 ± 0.0165	1.7131 ± 0.0170	<0.001	0.001	<0.001
VDI	5.4988 ± 0.1142	5.7384 ± 0.4629	5.8130 ± 0.1962	<0.001	0.003	0.447
Peripapillary RPCP (4.5mm × 4.5mm)						
VD, %	48.9200 ± 7.2317	46.5744 ± 7.9164	44.2640 ± 6.7874	0.055	0.173	0.227
VLF	0.0686 ± 0.0092	0.0641 ± 0.0104	0.0594 ± 0.0086	0.001	0.045	0.060
FD	1.6691 ± 0.0222	1.6632 ± 0.0281	1.6544 ± 0.0246	0.086	0.306	0.197
VDI	8.1853 ± 0.4239	8.4910 ± 0.6483	8.7830 ± 0.5648	<0.001	0.016	0.065

*P* < 0.05 was considered statistically significant difference between the groups.

SD, standard deviation; SQ, scan quality; PERIM, FAZ perimeter; FD-300, vessel density of a 300-µm width annulus surrounding FAZ; FD, fractal dimension.

\**P* value was calculated among the three DR groups (NoDR, NPDR and PDR)

†*P* value was calculated between NoDR and NPDR groups.

‡*P* value was calculated between NPDR and PDR groups.

### Multivariate Regression Model for OCTA Parameters

The ordinal regression model was used for the comparison of OCTA parameters among the three DR groups (NoDR, NPDR and PDR). VDI in the SCP (odds ratio [OR] 8.291, 95% CI [confidence interval] = 1.408–48.716, *P* = 0.019) and VD in the DCP (OR 0.982, 95% CI = 0.967–0.999, *P* = 0.037) showed the strongest positive correlation with severity of DR (Fig. 1).

The binary logistic regression model was used for the comparison of OCTA parameters between groups. EAA in the SCP was the strongest parameter that significantly discriminated between NoDR and NPDR eyes (OR 1.052, 95% CI = 1.017–1.088, *P* = 0.004) (Fig. 2). Receiver operating characteristic (ROC) curve of EAA (SCP) was generated and area under curve was 0.854 with sensitivity and specificity of 83.72% and 78.38%, respectively (Fig. 3). The same regression

analysis was performed for NPDR and PDR groups. VD in the DCP was the strongest parameter that significantly discriminated between these two groups (OR 0.975, 95% CI = 0.956–0.993, *P* = 0.008). The ROC curve showed an area under the curve of 0.827 with sensitivity and specificity of 84.00% and 79.07% respectively (Fig. 4).

The results of the multivariate regression model and ROC curve analysis are listed in Table 2.

### Discussion

In this study, we analyzed a total of 18 OCTA parameters in three retinal slabs (SCP, DCP, and RPCP) for each eye with severity of DR including four FAZ associated parameters (FAZ area, FAZ perimeter, AI, FD-300), five parameters for parafoveal SCP and DCP, respectively (EAA, VD, VLF, FD, and VDI), and four parameters for peripapillary RPCP (VD, VLF,

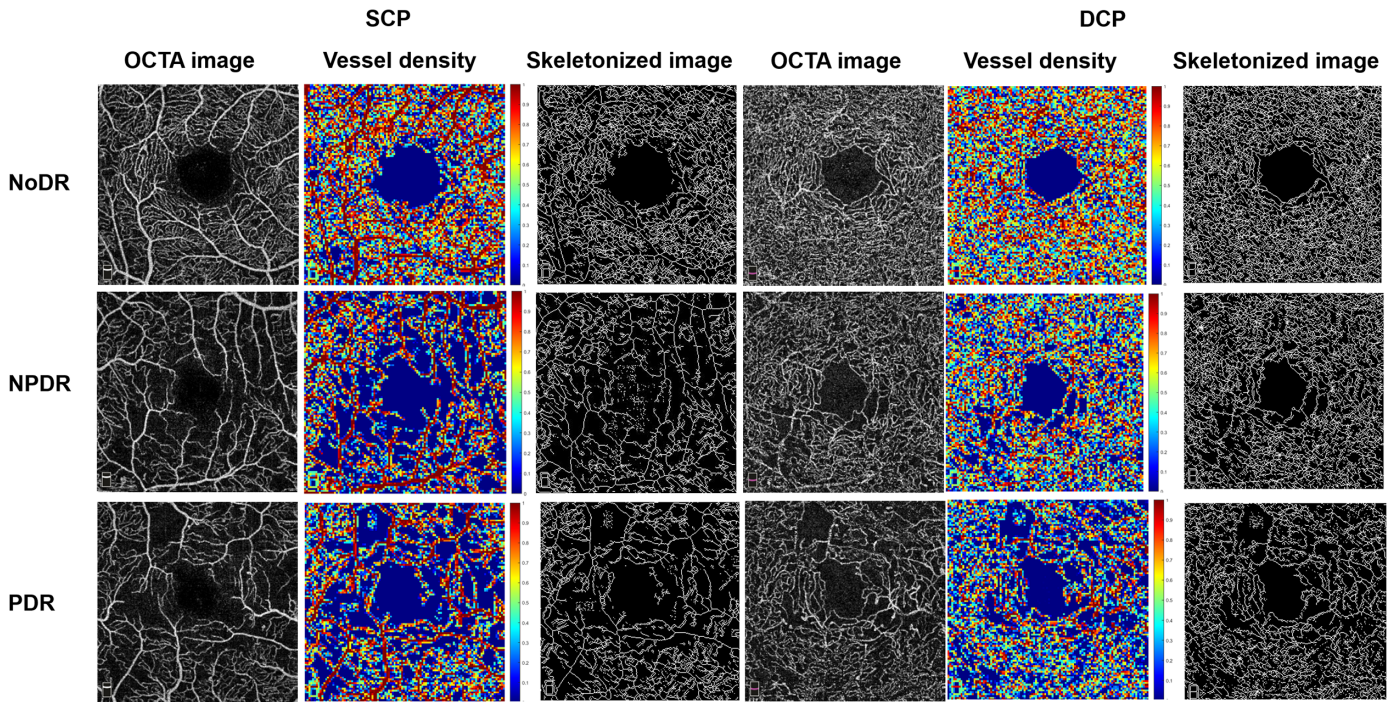


**Figure 1.** Analysis of the parafoveal microvascular changes in patients with different severity of diabetic retinopathy using segmented optical coherence tomography angiography images. Both SCP and DCP were studied. The VDI was calculated from the skeletonized images.

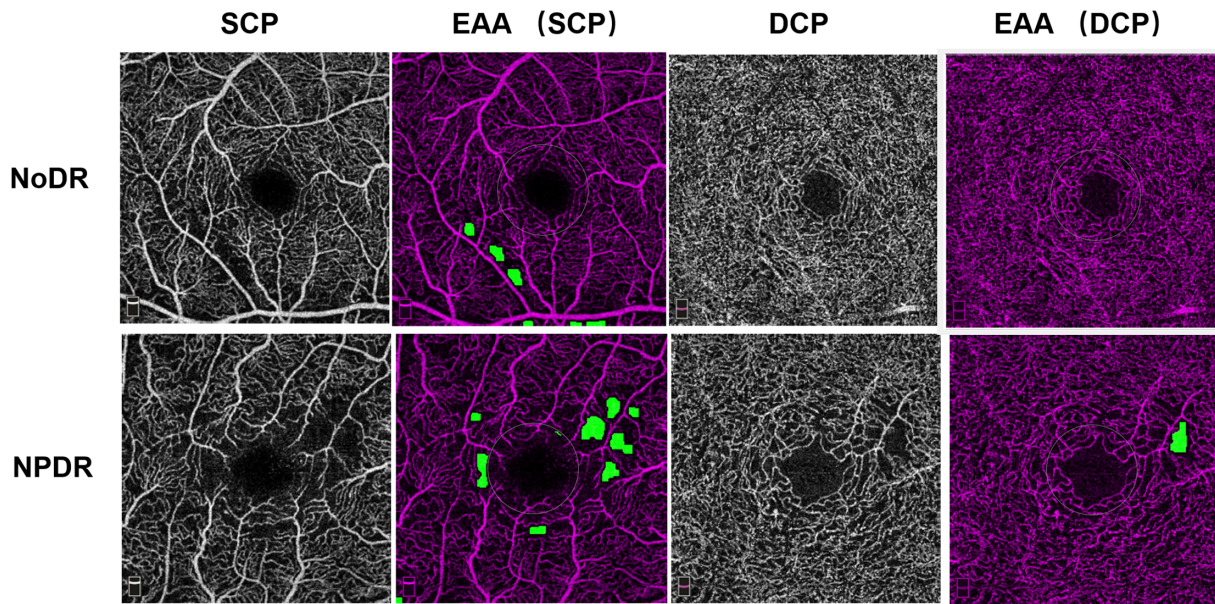


**Figure 2.** EAA was calculated in both parafoveal SCP and DCP for patients with NoDR and NPDR.

FD, and VDI). The multivariate ordinal regression model identified that VDI in the SCP and VD in the DCP are the strongest biomarkers that correlate with the severity of DR. The binary logistic regression model demonstrated that EAA in the SCP is the most sensitive biomarker to discriminate NoDR from NPDR eyes. Vessel density in the DCP is the most

sensitive parameter to distinguish eyes with NPDR from those with PDR.

OCTA as a noninvasive technique has been introduced to observe multiple retinal findings of DR from mild capillary drop out to retinal neovascularization.<sup>14,15</sup> Multiple ocular and systemic diseases such as glaucoma, Marfan syndrome, Fabry disease

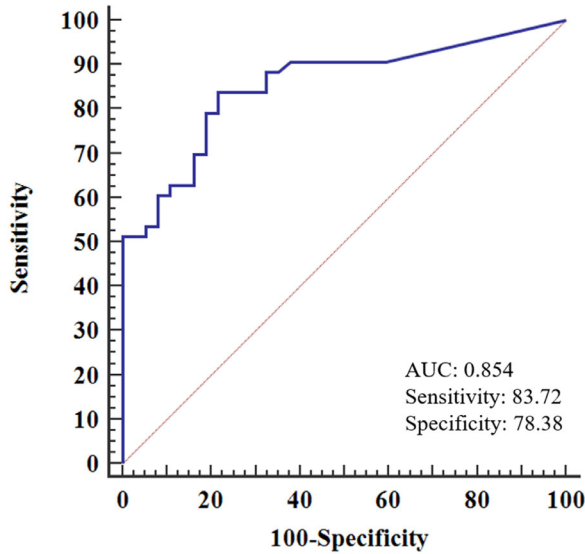


**Figure 3.** ROC curve of EAA in the SCP for eyes with NoDR versus NPDR.

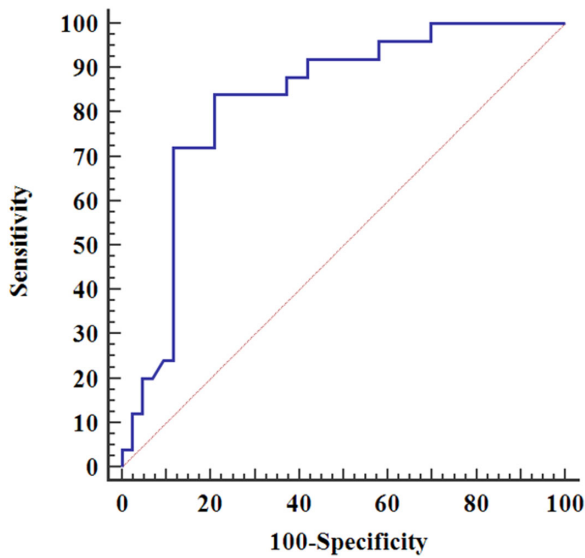


**Figure 4.** ROC curve of parafoveal VD in the DCP for eyes with NPDR versus those of PDR.

and Alzheimer’s diseases were evaluated with OCTA and found to be correlated with retinal microvascular changes.<sup>16–19</sup> With the improvement of projection artifact removal technique, the analysis of DCP becomes more accurate and reliable.<sup>20</sup> The 3 × 3 mm scans are better than 6 × 6 mm scans in some conditions because of the greater scan density and resolution, which could better delineate the FAZ and visualize retinal capillaries.<sup>20,21</sup> However, 6 × 6 mm scanning is also proven to be accurate and takes a larger retinal area.

FAZ metrics and vessel density are the most commonly investigated parameters in DR research. The FAZ area and the FAZ perimeter are not ideal biomarkers in the staging of DR because of the high variation among normal individuals but may have a prognostic role in predicting the DR progression, diabetic macular edema and visual acuity.<sup>22–26</sup> The FAZ AI has been reported to be significantly different between DR groups of severity but could not discriminate the diabetic eyes without clinical signs of DR from healthy controls.<sup>27</sup> On the contrary, FD-300 has been reported to be a sensitive biomarker for detecting microvascular changes in diabetic patients before the clinical sign of DR.<sup>28</sup> In our study, none of the FAZ metrics were of significance with severity of DR in the final model which indicates that the changes in the FAZ may not play an important role in advanced DR.

Decreased vessel density and increased area of nonperfusion in the parafoveal DCP were reported to be significantly correlated with DR severity and could predict the progression of DR suggesting the DCP is more vulnerable to damage than the SCP in diabetic patients.<sup>29,30</sup> A recent study which included patients with anti-VEGF and PRP treatment demonstrated that the decreased DCP vessel density was primarily present in absent to early DR, whereas in eyes with advanced DR, the alteration of VD was mainly found in the superficial layer.<sup>31</sup> A combined model of SCP FAZ area, DCP vessel density and acircularity was

**Table 2.** Comparison Between Groups Using Multivariate Regression Models and ROC Analysis of the Parameters that of Significance

	Logistic Regression			ROC Analysis		
	OR	95% CI	P	AUC	Sensitivity	Specificity
Parameters among the three DR groups (NoDR, NDPR and PDR)						
VDI (SCP)	8.281	1.408–48.716	0.019			
VD (DCP)	0.982	0.967–0.999	0.037			
Parameters between NoDR and NPDR groups, EAA (SCP)	1.052	1.017–1.088	0.004	0.854	83.72	78.38
Parameters between NPDR and PDR groups, VD (DCP)	0.975	0.956–0.993	0.008	0.827	84.00	79.07

P < 0.05 was considered statistically significant difference between the groups.  
AUC, area under the curve.

used to distinguish eyes with different severity of DR with a high ROC value.<sup>32</sup> In our study, VD in the DCP was strongly correlated with the severity of DR and was a sensitive biomarker to discriminate NPDR from PDR. This would indicate that loss of capillary density in the DCP may be an important pathological finding in the progression of DR, especially in the advanced stages.

In 2016, Bhanushali et al<sup>6</sup> observed a higher spacing between large vessels in the superficial layer in PDR and severe NPDR than in mild and moderate NPDR. EAA is a metric introduced recently to measure the extrafoveal avascular area outside the 1-mm central circle hence avoiding the problem of the normal variation of the FAZ. In addition, an area smaller than eight pixels vessel distance was not counted, which minimized the effect of the normal avascular area along retinal arterioles. EAA had been reported to have great sensitivity to differentiate diabetic eyes of all stages from healthy controls.<sup>10,25</sup> Specifically, EAA from SCP was reported to be the most sensitive biomarker to detect diabetic retinopathy of all stages.<sup>33</sup> The baseline DCP EAA was significantly correlated with worse visual acuity and treatment requirement in the one-year follow-up of DR, while the baseline superficial EAA was significantly associated with the progression of DR. In our study, compared to other microvascular metrics, the SCP EAA was the most sensitive parameter in detecting NPDR from NoDR. This indicates dropout of microvasculature in the SCP may play an important role in the early progression of DR. Neither SCP or DCP EAA showed significant difference between NPDR and PDR in the final multivariate model in our study.

VDI that measures the vessel caliber was known to react to hyperoxia but not to hypercapnia in the SCP of diabetic patients.<sup>34</sup> Increased VDI was identified in the SCP with increased severity of DR and moreover, was reported to be associated with photoreceptor loss and a higher fasting glucose level.<sup>35–37</sup> In our study, VDI in the SCP was strongly correlated with the severity of DR after multivariate ordinal regression analysis that indicated that VDI (SCP) may serve as a biomarker for the progression of DR.

The limitations in our study include the following: (1) In order to obtain a higher scan density and quality, small scan fields were observed, hence microvascular changes outside the parafoveal area and peripapillary area were not studied. (2) Patients with severe PDR may have some difficulties in obtaining high-quality images by OCTA. Those with diabetic macular edema were not included in our study. These may result in selection bias. (3) Systemic factors such as hypertension, hyperlipidemia, HbA1c level were not included in

this study. (4) NPDR was not graded into mild, moderate, or severe. (5) Axial length was not obtained though refractive errors in our patients were small.

In conclusion, we analyzed the FAZ, vessel density and vessel morphology associated with OCTA parameters in DR patients and compared them with severity of the DR. The SCP VDI and DCP VD are the strongest factors that related to the severity of DR. SCP EAA is the most sensitive biomarker to discriminate between NoDR from NPDR. In addition, DCP VD is the strongest biomarker to distinguish NPDR from PDR. OCTA could serve as a convenient and promising technique in observing the progression of DR at different stages.

## Acknowledgments

Supported by the National Natural Science Foundation of China (Grant No. 81971697, 81501544, 81200697), and Scientific Research Project of Hunan Provincial Health Commission (Grant No. 202107020970).

Disclosure: **X. Wang**, None; **Y. Han**, None; **G. Sun**, None; **F. Yang**, None; **W. Liu**, None; **J. Luo**, None; **X. Cao**, None; **P. Yin**, None; **F.L. Myers**, None; **L. Zhou**, None

\* XW and YH contributed equally to this work.

## References

1. Collaboration NCDRF. Worldwide trends in diabetes since 1980: a pooled analysis of 751 population-based studies with 4.4 million participants. *Lancet*. 2016;387:1513–1530.
2. Zheng Y, He M, Congdon N. The worldwide epidemic of diabetic retinopathy. *Indian J Ophthalmol*. 2012;60:428–431.
3. Cusick M, Chew EY, Chan CC, Kruth HS, Murphy RP, Ferris FL, 3rd. Histopathology and regression of retinal hard exudates in diabetic retinopathy after reduction of elevated serum lipid levels. *Ophthalmology*. 2003;110:2126–2133.
4. Grauslund J, Andersen N, Andresen J, et al. Evidence-based Danish guidelines for screening of diabetic retinopathy. *Acta Ophthalmol*. 2018;96:763–769.
5. Spaide RF, Fujimoto JG, Waheed NK, Sadda SR, Staurenghi G. Optical coherence tomography angiography. *Prog Retin Eye Res*. 2018;64:1–55.

6. Bhanushali D, Anegondi N, Gadde SG, et al. Linking retinal microvasculature features with severity of diabetic retinopathy using optical coherence tomography angiography. *Invest Ophthalmol Vis Sci.* 2016;57:OCT519–OCT525.
7. De Pretto LR, Moulton EM, Alibhai AY, et al. Controlling for artifacts in widefield optical coherence tomography angiography measurements of non-perfusion area. *Sci Rep.* 2019;9:9096.
8. Hormel TT, Huang D, Jia Y. Artifacts and artifact removal in optical coherence tomographic angiography. *Quant Imaging Med Surg.* 2021;11:1120–1133.
9. Li C, Xu C, Gui C, Fox MD. Distance regularized level set evolution and its application to image segmentation. *IEEE Trans Image Process.* 2010;19:3243–3254.
10. Zhang M, Hwang TS, Dongye C, Wilson DJ, Huang D, Jia Y. Automated quantification of non-perfusion in three retinal plexuses using projection-resolved optical coherence tomography angiography in diabetic retinopathy. *Invest Ophthalmol Vis Sci.* 2016;57:5101–5106.
11. Pappelis K, Jansonius NM. Quantification and repeatability of vessel density and flux as assessed by optical coherence tomography angiography. *Transl Vis Sci Technol.* 2019;8:3.
12. Pappelis K, Choritz L, Jansonius NM. Microcirculatory model predicts blood flow and autoregulation range in the human retina: in vivo investigation with laser speckle flowgraphy. *Am J Physiol Heart Circ Physiol.* 2020;319:H1253–H1273.
13. Reishofer G, Koschutnig K, Enzinger C, Ebner F, Ahammer H. Fractal dimension and vessel complexity in patients with cerebral arteriovenous malformations. *PLoS One.* 2012;7:e41148.
14. Russell JF, Flynn HW, Jr., Sridhar J, et al. Distribution of diabetic neovascularization on ultra-widefield fluorescein angiography and on simulated widefield OCT angiography. *Am J Ophthalmol.* 2019;207:110–120.
15. Zhang B, Chou Y, Zhao X, Yang J, Chen Y. Early detection of microvascular impairments with optical coherence tomography angiography in diabetic patients without clinical retinopathy: a meta-analysis. *Am J Ophthalmol.* 2021;222:226–237.
16. Chua J, Hu Q, Ke M, et al. Retinal microvasculature dysfunction is associated with Alzheimer's disease and mild cognitive impairment. *Alzheimers Res Ther.* 2020;12:161.
17. Di Marino M, Cesareo M, Aloe G, et al. Retinal and choroidal vasculature in patients with Marfan syndrome. *Transl Vis Sci Technol.* 2020;9:5.
18. Martucci A, Giannini C, Di Marino M, et al. Evaluation of putative differences in vessel density and flow area in normal tension and high-pressure glaucoma using OCT-angiography. *Prog Brain Res.* 2020;257:85–98.
19. Minnella AM, Barbano L, Verrecchia E, et al. Macular impairment in Fabry disease: a morpho-functional assessment by swept-source OCT angiography and focal electroretinography. *Invest Ophthalmol Vis Sci.* 2019;60:2667–2675.
20. Binotti WW, Romano AC. Projection-resolved optical coherence tomography angiography parameters to determine severity in diabetic retinopathy. *Invest Ophthalmol Vis Sci.* 2019;60:1321–1327.
21. Ho J, Dans K, You Q, Nudleman ED, Freeman WR. Comparison of 3 mm x 3 mm versus 6 mm x 6 mm optical coherence tomography angiography scan sizes in the evaluation of non-proliferative diabetic retinopathy. *Retina.* 2019;39:259–264.
22. Sun Z, Tang F, Wong R, et al. OCT angiography metrics predict progression of diabetic retinopathy and development of diabetic macular edema: a prospective study. *Ophthalmology.* 2019;126:1675–1684.
23. Linderman RE, Muthiah MN, Omoba SB, et al. Variability of foveal avascular zone metrics derived from optical coherence tomography angiography images. *Transl Vis Sci Technol.* 2018;7:20.
24. Atta Allah HR, Mohamed AAM, Ali MA. Macular vessels density in diabetic retinopathy: quantitative assessment using optical coherence tomography angiography. *Int Ophthalmol.* 2019;39:1845–1859.
25. Lu Y, Simonett JM, Wang J, et al. Evaluation of automatically quantified foveal avascular zone metrics for diagnosis of diabetic retinopathy using optical coherence tomography angiography. *Invest Ophthalmol Vis Sci.* 2018;59:2212–2221.
26. Custo Greig E, Brigell M, Cao F, et al. Macular and peripapillary optical coherence tomography angiography metrics predict progression in diabetic retinopathy: a sub-analysis of TIME-2b study data. *Am J Ophthalmol.* 2020;219:66–76.
27. Krawitz BD, Mo S, Geyman LS, et al. Acircularity index and axis ratio of the foveal avascular zone in diabetic eyes and healthy controls measured by optical coherence tomography angiography. *Vision Res.* 2017;139:177–186.
28. Ragkousis A, Kozobolis V, Kabanarou S, et al. Vessel density around foveal avascular zone as a potential imaging biomarker for detecting pre-clinical diabetic retinopathy: an optical coherence



- tomography angiography study. *Semin Ophthalmol*. 2020;35:316–323.
29. Nesper PL, Roberts PK, Onishi AC, et al. Quantifying microvascular abnormalities with increasing severity of diabetic retinopathy using optical coherence tomography angiography. *Invest Ophthalmol Vis Sci*. 2017;58:BIO307–BIO315.
  30. Rodrigues TM, Marques JP, Soares M, et al. Macular OCT-angiography parameters to predict the clinical stage of nonproliferative diabetic retinopathy: an exploratory analysis. *Eye (Lond)*. 2019;33:1240–1247.
  31. Ashraf M, Sampani K, Clermont A, et al. Vascular density of deep, intermediate and superficial vascular plexuses are differentially affected by diabetic retinopathy severity. *Invest Ophthalmol Vis Sci*. 2020;61:53.
  32. Ashraf M, Nesper PL, Jampol LM, Yu F, Fawzi AA. Statistical model of optical coherence tomography angiography parameters that correlate with severity of diabetic retinopathy. *Invest Ophthalmol Vis Sci*. 2018;59:4292–4298.
  33. Hwang TS, Hagag AM, Wang J, et al. Automated quantification of nonperfusion areas in 3 vascular plexuses with optical coherence tomography angiography in eyes of patients with diabetes. *JAMA Ophthalmol*. 2018;136:929–936.
  34. Singer M, Ashimatey BS, Zhou X, Chu Z, Wang R, Kashani AH. Impaired layer specific retinal vascular reactivity among diabetic subjects. *PLoS One*. 2020;15:e0233871.
  35. Weisner G, Blindbaek SL, Tang FY, et al. Non-invasive structural and metabolic retinal markers of disease activity in non-proliferative diabetic retinopathy [published online ahead of print January 8, 2021]. *Acta Ophthalmol*, <https://doi.org/10.1111/aos.14761>.
  36. Lei J, Xu X, Chen L, Fan X, Abdelfattah NS. Dilated retinal large vessels and capillaries associated with diabetic macular edema and photoreceptor loss respectively [published online ahead of print January 8, 2021]. *Graefes Arch Clin Exp Ophthalmol*, <https://doi.org/10.1007/s00417-020-05039-2>.
  37. Tang FY, Ng DS, Lam A, et al. Determinants of quantitative optical coherence tomography angiography metrics in patients with diabetes. *Sci Rep*. 2017;7:2575.